Medical Oncology (2023) 40:126
https://doi.org/10.1007/s12032-023-01991-1

ORIGINAL PAPER

Gold cluster encapsulated liposomes: theranostic agent with stimulus triggered release capability

Seyed Mohammad Amini[1,2] · Seyed Mahdi Rezayat[2,3] · Rassoul Dinarvand[4] · Sharmin Kharrazi[2] · Mahmoud Reza Jaafari[5,6]

Received: 28 January 2023 / Accepted: 7 March 2023 / Published online: 24 March 2023

Abstract

Cancer is a major cause of death worldwide. Cancer-resistant to chemo or radiotherapy treatment is a challenge that could be overcome by a nanotechnology approach. Providing a theranostic nano-platform for different cancer treatment strategies could be revolutionary. Here we introduce a multifunctional theranostic nanostructure which has the capacity for improving cancer diagnosis and treatment through better chemo and radiotherapy and current x-ray imaging systems through co-encapsulation of a small gold cluster and anticancer drug doxorubicin. 2 nm gold clusters represent good heating under radio frequency electric field (RF-EF) exposure and have been used for in vitro hyperthermia treatment of cancerous cells. Liposomal doxorubicin (169 ± 19.8 nm) with gold clusters encapsulation efficiency of 13.2 ± 3.0% and doxorubicin encapsulation efficiency of 64.7 ± 0.7% were prepared and studied as a theranostic agent with a high potential in different cancer treatment modalities. Exposure to a radiofrequency electric field on prepared formulation caused 20.2 ± 2.1% drug release and twice decreasing of IC50 on colorectal carcinoma cells. X-ray attenuation efficiency of the liposomal gold cluster was better than commercial iohexol and free gold clusters in different concentrations. Finally, treatment of gold clusters on cancerous cells results in a significant decrease in the viability of irradiated cells to cobalt-60 beam. Based on these experiments, we concluded that the conventional liposomal formulation of doxorubicin that has been co-encapsulated with small gold clusters could be a suitable theranostic nanostructure for cancer treatment and merits further investigation.

Keywords Gold clusters · Liposomes · Theranostic agents · Trigger release · Radio frequency electric field · Radiation therapy · X-ray contrast agent

Introduction

Radiotherapy and chemotherapy are the most common treatments for different cancers besides surgery. In fact, a combination of both has been found effective in various cancers [1]. Despite significant advances in systemic chemotherapy of solid tumours, there are many challenges remain in this area that makes this treatment almost unable to reach a therapeutic level of anticancer drug in tumour site without significant side effect [2]. Apart from other applications like biosensor [3], nanostructures are applied in the field of oncology for both therapeutic and diagnostic applications as

✉ Sharmin Kharrazi
Sh-kharrazi@tums.ac.ir

✉ Mahmoud Reza Jaafari
jafarimr@mums.ac.ir

1 Radiation Biology Research Center, Iran University of Medical Sciences (IUMS), Tehran, Iran

2 Department of Medical Nanotechnology, School of Advanced Technologies in Medicine (SATiM), Tehran University of Medical Sciences (TUMS), Tehran, Iran

3 Department of Pharmacology, School of Medicine, Tehran University of Medical Sciences, Tehran, Iran

4 Nanotechnology Research Centre, Novel Drug Delivery Department, Faculty of Pharmacy, Tehran University of Medical Sciences, Tehran, Iran

5 Pharmaceutical Technology Institute, School of Pharmacy, Nanotechnology Research Center, Mashhad University of Medical Sciences, 91775-1365 Mashhad, Iran

6 Department of Pharmaceutical Nanotechnology, School of Pharmacy, Mashhad University of Medical Sciences, 91775-1365 Mashhad, Iran

a theranostic agent or a multi-platform for different therapeutics treatment [4].

Potential harm to normal tissues in the path of the ionizing beam was the main limitation of radiotherapeutic treatment of cancers. Nanoparticles as radiosensitizers could be applied to enhance radiation effects in tumour cells and decrease the patient radiation doses [5]. High-Z dose nanoparticle such as gold [6], silver [7], germanium [8], platinum [9] or bismuth [10] introduced as cancer radio sensitization agents. Amongst them, the number of reports on gold nanoparticles radiosensitization or x-ray imaging applications has rapidly increased because of their relatively inert property, biocompatibility, simple synthesis and ease in the chemical modification [4–6, 11]. Based on Chithrani et al. report 50 nm gold nanoparticles are better radio sensitizer because of higher cellular uptake in comparison to smaller particles [11]. Gold nanoparticles isn't metabolized, and due to their large size, they prefer to accumulate in the liver and spleen. The gold clusters with the small size can penetrate kidney tissue and could be removed by renal clearance [12]. Delivery of gold cluster through injection in tumour area is a major challenge because of their wide biodistribution [13, 14].

Amongst differently designed nanocarriers to achieve cancer drug delivery with reduced systemic side effects, the pegylated liposome is the most important one that has been approved for application of some anti-cancer drugs like doxorubicin in myeloma, aids-related Kaposi's sarcoma and ovary or breast cancer treatment [15, 16]. Pegylated liposomal doxorubicin still shows no or very low activity against many common cancers, such as sarcoma, non–small-cell lung cancer and hepatoma [17, 18]. The main problem is that doxorubicin is not available to the tumour cells whilst liposomal doxorubicin is accumulated in the tumour region. So liposomal doxorubicin accumulation is higher in comparison to non-encapsulated doxorubicin [19].

Pegylated liposomal doxorubicin formulations can extravasate tumour endothelium and accumulate in a tumour extracellular spaces, but long chain surface poly ethylene glycol (PEG) and bilayer toughness retard fusion or uptake of the liposomes by cancerous cells [20–22]. There are two strategies to overcome this challenge. Active drug delivery with the help of different biomolecules leads to receptor-mediated endocytosis of ligand-targeted liposomes [23, 24]. This recipe is not only too expensive and needs a lot of effort to develop a new drug for every type of cancer cell but also might not be effective because of cancer proteome variation. The second strategy is the developing stimulus-responsive liposomal formulation for the trigger release of drug content in solid tumour space.

Liposomes, stability in circulation helps the retention of loaded drug and decrease the systemic side effect as well as better drug delivery. Trigger release of liposome contents in the tumour site was usually achieved with two different methods. Intrinsic stimulus in the site of tumours like enzymes, salt concentration and pH changes and external stimuli such as heat, light and ultrasound has been reviewed comprehensively. In most of these methods, lipid composition changed dramatically after external stimuli exposure that leads to unwanted leakage of drugs [25].

Here we report a new stimulus to trigger the release of doxorubicin from the liposomal formulation containing gold clusters. We report on the design, development and investigation of doxorubicin release under radiofrequency electric field exposure of pegylated liposomes containing gold clusters. The lipid composition was the same as the commercially-available Doxil® formulation for stable liposome formulation of doxorubicin with minimum unwanted leakage of the drug that may cause a systemic side effect. Besides the capability in hyperthermia and effective chemotherapy, the Au cluster encapsulated in pegylated liposomes could be a great x-ray contrast agent for computed tomography and a radiosensitization agent for combination radiotherapy and chemotherapy treatment of cancer. A schematic view of the capability of the Au cluster encapsulated in pegylated liposomes which have been studied in this paper was drawn in Fig. 1.

Materials and methods

Materials

Chloroauric acid ($HAuCl_4 \cdot 3H_2O$, 99.5%), mercaptosuccinic acid ($C_4H_6O_4S$, 98%), sodium borohydride ($NaBH_4$, 98%), hydrochloric acid (HCl reagent, 37%), nitric acid (HNO_3 reagent, 65%), ethanol, chloroform and methanol were purchased from Merck (Germany). Cholesterol (Chol), Methoxypolyethylene glycol (MW 2000)–distearoylphosphatidylcholine (mPEG2000–DSPE), hydrogenated soy phosphatidylcholine (HSPC) and COOH-PEG2000-DSPE were obtained from Avanti Polar Lipids (Alabaster, AL). By adding 7.5 mL HCl 1 M and 2.5 mL water to 90 mL isopropanol (Merck, Germany) acidified isopropyl alcohol (90% isopropanol/0.075 M HCl) was prepared. C-26 colon carcinoma cells were purchased from Cell Lines Service (Eppelheim, Germany). Fetal bovine serum (FBS), RPMI 1640 culture medium, penicillin and streptomycin were obtained from Gibco. MTT (thiazolyl blue tetrazolium bromide) dye and dimethyl sulfoxide (DMSO) were obtained from Sigma-Aldrich (Germany). All solutions were prepared with DI water (Barnsted E-PureTM 18.3 MΩ). Glasswares were cleaned with aqua regia and rinsed thoroughly with DI water.

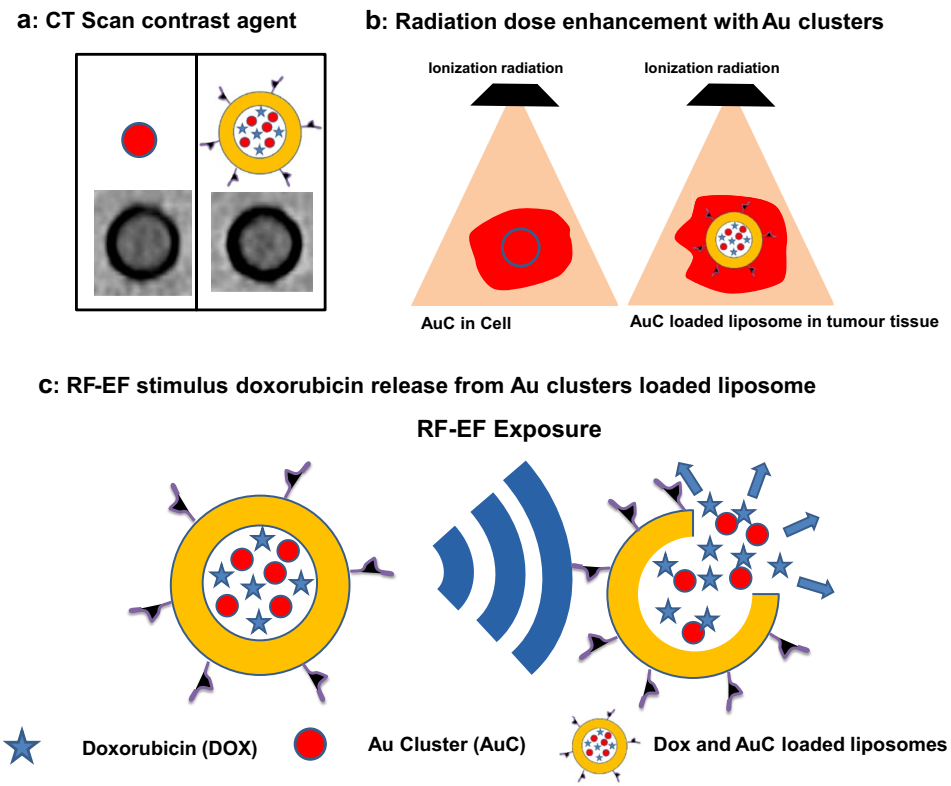

Fig. 1 A schematic view of the theranostic applications of the gold cluster (AuC) and doxorubicin (Dox) loaded liposomes. Due to the high atomic number of gold, gold clusters and liposomes containing gold clusters could be used in computed tomography (CT scan) as a contrast agent (**a**). Gold cluster loaded liposomes could reach the tumour site and deliver the gold clusters to the cancer cells. Both of the nanostructures could increase the absorbed dose and improve the radiation therapy efficiency (**b**). Exposure of RF-EF on encapsulated gold cluster could lead to higher Dox release from liposomal formulation and improve the chemotherapy efficiency (**c**)

Synthesis of gold clusters

Gold clusters with an average size of 2 nm have been synthesized based on our previous reports [26]. Briefly, 0.5 mMol of gold salt ($HAuCl_4 \cdot 3H_2O$) in DI water was mixed with 1.25 mMol Mercaptosuccinic acid (MSA) in 100 mL of methanol. After adding 25 mL of ice-cold and fresh $NaBH_4$ (0.2 M) reduced gold precipitate can be found in the solution. After 1 h precipitate was separated by centrifugation and redispersed in water/methanol (20% v/v) using sonication. The same procedure was performed with pure methanol twice and finally dispersed in pure ethanol. This solution was dried through a rotary evaporator and the resulting powder was dispersed in DI water and dialyzed with a 12 kDa cellulose dialysis bag.

Encapsulated gold clusters in liposomal doxorubicin

Briefly, from stock solutions, HSPC, mPEG2000-DSPE and cholesterol were added to a glass tube in molar percentage ratios of 55:40:5. Through a rotary evaporator, lipids were dried. Then the remaining chloroform was evaporated with a 2 h connection to a freeze-dryer. Liposomes were prepared by thin lipid film hydration and downsized by sonication and extrusion [27]. The prepared lipid film was hydrated in a solution of ammonium sulphate (250 mM) and gold clusters (different concentrations) at 65 °C under an argon atmosphere, sonicated for 20 min and then extrusion followed through polycarbonate membranes of 400 nm, 200 nm and 100 nm, in sequence. To remove free gold clusters and ammonium sulphate ions liposomes were dialyzed against 5% w/v dextrose solution. The mass of total lipid concentration was determined by phospholipid assay based on Bartlett phospholipid assay [28]. Using the ammonium sulphate gradient technique, doxorubicin was encapsulated in liposomes through a remote loading technique based on previous reports [29, 30]. Liposomes with encapsulated ammonium sulphate were incubated with doxorubicin solution (2 mg doxorubicin per 10 µmol of total lipid) at 65 °C for 1 h, cooled to room temperature, mixed with Dowex® resin and rotated for 1 h to remove free doxorubicin. Liposomes were then filter sterilized using a 0.22 µm microbial filter and kept at 4 °C for future usage. Doxorubicin concentration was calculated by fluorometry (excitation 470 nm-emission 550 nm) [31].

Characterization of gold clusters and clusters loaded liposome

UV- visible absorption spectroscopy has been performed with 1 cm of optical path length quartz cuvette (SPEKOL 2000 double beam UV–visible spectrophotometer (Analytik Jena, UK)). Average hydrodynamic diameter and polydispersity index (PDI) was investigated in triplicate

measurement by a dynamic light scattering particle size analyzer (Qudix Scatteroscope I, South Korea). The size distribution was calculated by the following formulation.

$$S.D. = \frac{\sqrt{D75}}{\sqrt{D25}}$$

Malvern Nanosizer (Malvern Instrument, UK) has been used for Zeta potential measurement in neutral pH. The samples have been prepared in 5% w/v dextrose buffer. Throughout this article, we are addressing the concentration of gold atoms, which has determined by using inductively coupled plasma atomic emission spectroscopy ((ICP-AES) (VISTA-PRO, Varian, Australia)). To prepare ICP-AES samples, the gold cluster or liposomal formulation of the gold cluster was poured to a volumetric flask of aqua regia ($1HNO_3 + 3HCl$) and placed on a heater at 70 °C. The heating continued up to 2 h. After adjusting the volume with DI water, the measurements were conducted in triplicate and the mean ± SD of the results were calculated and reported.

Spectrofluorometer (Jasco FP-6200, USA) has been used for doxorubicin concentration measurements. TEM micrographs of gold clusters were recorded by Hitachi HF-3300 ETEM/STEM at 300 kV. TEM micrographs of gold clusters encapsulated liposomes were recorded by Zeiss EM 900 microscope operated at 80 kV without any staining. TEM samples have been prepared by adding 30 µl of gold cluster (200 µg/mL) and gold cluster loaded liposomes (At initial Au concentration of 2700 µg/mL) solution onto 300-mesh carbon-coated copper grids and allowed to dry.

X-ray attenuation assay

A cylinder-designed scanning holder (Poly(methyl methacrylate)(PMMA)) resin was used for computed tomography (CT scan) imaging of iohexol (OMNIPAQUE™), gold cluster and gold cluster encapsulated liposomes with a CT imaging system (SOMATOM Scope, Siemens). CT scan parameters including tube current: 125 mAs (milliampere. second), tube voltage: 80 kVp (peak kilovoltage) and slice thickness: 1 cm fixed based on previous reports [4, 32]. Three equal concentrations of gold clusters and gold cluster loaded liposomes were chosen for this experiment. Water-filled and empty microtube were applied as negative control samples. Iohexol in different concentrations was used as positive control groups. X-ray attenuation of different contrast agents was measured by selecting a uniform ellipse region of interest (ROI) on the digital CT images of the sample. Contrast resolutions for each sample were evaluated and represented in Hounsfield units (HU).

Encapsulation efficiency analysis

Encapsulation efficiency of liposome formulation was investigated after removing released doxorubicin with Dowex® resin [31]. A standard curve of acidified isopropyl alcohol solution of doxorubicin has been prepared by fluorometry (excitation 470 nm-emission 550 nm). After liposomes lysis with acidified isopropyl alcohol, doxorubicin concentration was extrapolated according to the obtained standard curve. Encapsulation efficiency was calculated based on followed formula (each experiment has been repeated 3 times).

$$\text{Encapsulation efficiency} = \frac{\text{Doxorubicin Conc. after Dowex purification}}{\text{Doxorubicin Conc. before Dowex purification}} \times 100$$

RF-EF exposure experiment

RF-EF set up with the power of 100 Watts and at a frequency of 13.56 MHz was adapted for RF-EF exposure (Basafan Company, Tehran, Iran). Characteristics of RF-EF set up with a schematic representation and picture are reported in our previous report [26]. Each triplicate of a sample has exposure for 3 min in 1.5 mL microtubes. Release measurement and cell treatment were performed after RF-EF exposure of samples. The sample temperature and heating rate were measured using a pyrometer (Optex non-contact thermometer, SA-80 T-4A).

Doxorubicin stimulus release analysis

Stimulus release of doxorubicin was investigated in 2 different strategies. At first gold clusters and doxorubicin encapsulated liposomes was treated at different temperature with a warm water bath. Incubation was carried out for 1 h. Released doxorubicin from liposomes was removed by incubation of each sample with an appropriate quantity of Dowex resin as mentioned in Section "Encapsulated Gold Clusters in Liposomal Doxorubicin". The percentage of the remaining doxorubicin inside the liposomal formulation was calculated by the method that has been provided in Section "Encapsulation Efficiency Analysis". At last doxorubicin release under RF-EF exposure was performed with threefold diluted solution of prepared formulation in 5% w/v dextrose and provided stock formulation similar to the described method.

Cell studies

C-26 cells were cultured at 37 °C in RPMI 1640 medium supplemented with 10% (v/v) FBS, and 1% penicillin/

streptomycin with standard condition (5% CO_2, in the air-humidified atmosphere). To investigate the radiosensitization activity of gold clusters, 4000 Cells were seeded into each well of a 96-well plate and after 24 h cells were treated with a new culture medium containing a specific concentration of gold clusters. Cells were incubated for another 24 h and then each well was washed with PBS and filled with fresh culture medium before irradiation. The irradiation of different groups of cells was carried out by delivering 2 and 4 Gy of γ–rays using a Co-60 therapy machine. 24 h postirradiation, a MTT assay was performed to measure cell viability percentage.

To investigate the cytotoxic effect of treatment with different doxorubicin formulation treatment, 4000 Cells were seeded into each well of a 96-well plate and after 24 h cells were treated with a new culture medium containing a specific concentration of doxorubicin formulation. Cells were incubated for 3 h then each was washed with PBS and subsequently filled with fresh culture medium and incubated for another 48 h. In the end, the MTT assay was carried out.

MTT assay

Cells with different treatments were incubated with 100 µl, 0.5 mg/mL MTT in RPMI 1640 culture medium solution for 2–4 h under standard condition (5% CO_2, in the air-humidified atmosphere) then replaced with 100 µl DMSO. The absorption value of each well was read at the wavelength of 570 nm.

Statistical analysis

Data were plotted and analysed using Origin 2015 (OriginLab Co., USA), CalcuSyn version 2 (BIOSOFT, UK) and GraphPad Prism 6 (GraphPad Software, San Diego, CA) software. Data are shown as the mean ± standard deviation. Statistical significance, α, was set to $p < 0.05$. Groups were compared with one-way analysis of variances (ANOVA) unless it is noted. For the determination of half maximal inhibitory concentration (IC50), nonlinear regression analyses were performed.

Results and discussion

Characterization of gold cluster and gold cluster loaded liposomes

UV–Vis absorbance spectroscopy was applied to confirm the formation of clusters and their presence in liposomes (Fig. 2a). The absence of a typical SPR peak in UV–Vis absorbance spectra is an indication that clusters are smaller than 3 nm in size.

UV–Vis spectra do not represent any surface resonance plasmonic peak for gold clusters or encapsulated gold clusters inside liposomes (Fig. 2a). Based on our previous report, and presented HRTEM micrographs reveal semi-spherical morphology for a single crystalline gold cluster with a size of 2 ± 1.5 nm (Fig. 2b) [26]. For TEM analysis, liposomes were prepared with highly concentrated gold clusters solution (Initial Au concentration for liposome preparation was 2700 µg/mL), so there is no need for staining because of the high number of gold clusters that were encapsulated inside liposomes.

The extrusion procedure of these liposomes with high Au content was difficult to do. So for downstream experiments, we use lower concentrations of gold. Based on obtained micrographs clearly, dialysis removed most of the un-encapsulated gold clusters but free clusters could be found in TEM micrographs which is pointed with the red arrow in Fig. 2d. With decreasing the initial concentration of gold cluster and increasing the dialysis time amount of these free gold clusters would decrease.

Lipid film hydration for encapsulating nanoparticles inside the liposome hydrophilic core was investigated by many researchers [33–35]. But in many of them removing free particles was a challenge. Pradhan et al. encapsulated magnetic nanoparticles inside liposome with the same technique except for removing free nanoparticles which Sephadex G50 gel for size exclusion chromatography has been used but the number of free and aggregated particles found in provided TEM micrographs are more than encapsulated particles [33]. Lorenzato et al. reach a much better result with Sephadex S1000 gel for removing 5 nm magnetic nanoparticles [34]. PD 10 gel was used for removing free gold nanoparticles from liposomes encapsulated gold nanoparticles in Mathiyazhakan et al. In their report, gold nanoparticles were encapsulated inside liposomes or associated with lipid surfaces but free particles could be seen in provided TEM micrograph [36]. The amount of encapsulated magnetic or gold nanoparticles in mentioned reports is very few in comparison with our results.

Zeta potential and hydrodynamic diameters of cluster loaded liposomes are heavily dependent on the initial concentration of gold clusters (Table 1). A high initial concentration of gold clusters leads to a bigger hydrodynamic size for papered liposomes. This is probably the result of gold clusters' interference in extrusion efficacy. Higher hydrodynamic sizes were reported for liposome loaded nanoparticles in comparison to unloaded liposomes [33, 37, 38]. A similar situation was observed in Zeta potential investigation. Both liposomes and gold clusters are negatively charged so free gold clusters could be in higher quantities in liposomes samples with a high initial concentration of gold clusters. These clusters could be absorbed into the liposomal surface and increased the liposomes' negative charge (Table 1).

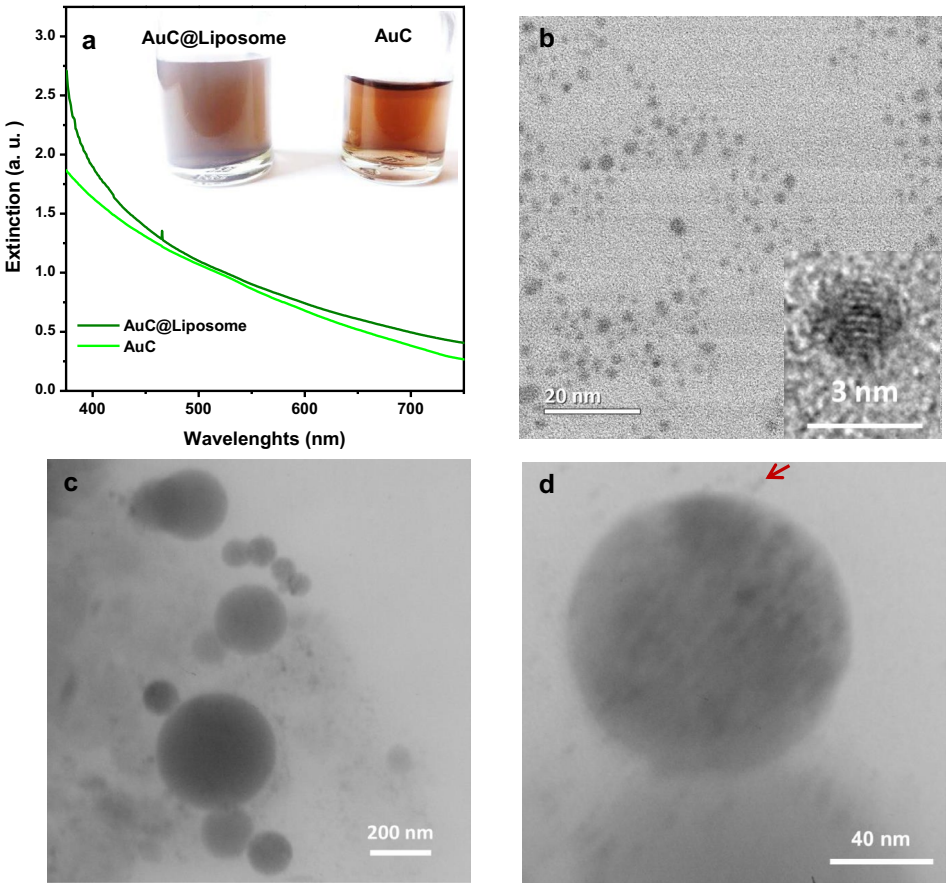

Fig. 2 UV–Vis absorption spectra and optical image of MSA capped gold clusters (AuCs) and gold cluster loaded liposomes (AuC@liposomes) (**a**). HR-TEM micrographs of MSA capped gold clusters (**b**) TEM micrographs of gold cluster loaded liposomes with initial Au concentration of 2.7 mg/mL (**c**). A separate micrograph of a gold cluster loaded liposome (**d**). Red arrow pointing at a free gold cluster

Table 1 Characterizations of gold cluster loaded liposomes

Liposomes sample (initial Au Conc.) (μg/mL)	Zeta potential (mV) (Mean ± SD)	Hydrodynamic diameter (nm) (Mean ± SD)	PDI (Mean ± SD)
S_1 (1500)	− 25.8 ± 0.6	260 ± 32.45	1.46 ± 0.14
S_2 (1000)	− 23.6 ± 1.1	184 ± 18.08	1.98 ± 0.13
S_3 (500)	− 16.3 ± 3.1	169 ± 19.80	1.52 ± 0.17
S_4 (0)	− 16.6 ± 5.0	120 ± 4.28	1.15 ± 0.02

Based on ICP-AES analysis, regardless of the initial amount of gold clusters for liposomes preparation, the average percentage of gold cluster encapsulation is 14.3 ± 2.2%. Initial gold concentration does not affect the loading efficiency in our experiment (no significant difference was observed).

Computed tomography scan

CT scan is one of the techniques that is used for the evaluation of colorectal carcinoma staging in clinics [39, 40]. Currently, high osmolar Iodine based molecules are the most common x-ray contrast agent in the clinic [41]. In several reports by various research groups, some nanoparticles were introduced as a contrast agent. Gold nanoparticles [4, 42], bismuth-based nanoparticles [43, 44] and up-conversion nanoparticles that contain inner transition metals [45, 46] were such agents.

As represented in Fig. 3 in 95 and 365 μg/mL concentrations, no significant differences were observed between the gold cluster and iohexol but in 525 μg/mL concentration, the gold cluster is a better x-ray absorbent in comparison to iohexol. The atomic number of gold (79) is much higher than iodine (53) but in very low concentrations, our CT imaging technic is not able to distinguish between the two groups.

Photoelectric absorption intensity is a function of gold nanoparticles' size. Because it follows a radius-cubed relation. Therefore nearly four orders of magnitude increase in photoelectric absorption were observed between 5 and

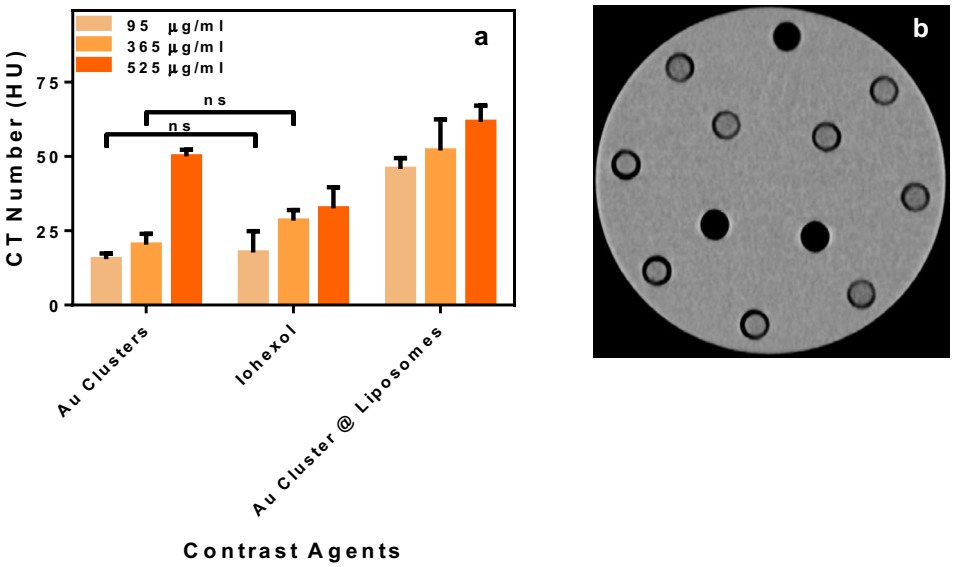

Fig. 3 X-ray attenuation (HU) intensity of iohexol (omnipaque), gold cluster and gold cluster loaded liposomes at different concentrations and same kVp (**a**). A two-way analysis of variance has been performed for statistical analysis of results (ns: not significant). One of the axial CT images of samples in the designed scanning holder (Poly (methyl methacrylate) (PMMA)) (**b**)

100 nm gold nanoparticles by Lechtman et al. [47]. Based on this gold cluster encapsulated liposomes represent higher HU in all three concentrations in comparison to the free gold cluster (Fig. 3a).

Irradiation of C-26 cells with Co-60 machine

Low-energy photon beams were suggested in many reports for in vitro radiosensitization investigation. Irradiating gold nanoparticles with kilovoltage x-ray photons greatly increased the number of secondary electrons and subsequently higher radiosensitization effect would be observed [48–50]. Kilovoltage therapy x-ray units penetrate tissue to a useful depth of about 4–6 cm and are applicable for superficial cancers [51]. Also, secondary electrons generated by irradiated gold nanoparticles with a high-energy cobalt-60 photon beam could travel greater distances [50] which may be important for encapsulated gold nanoparticles inside pegylated liposomal.

We use MTT assay because it has been used for cytotoxicity analysis of gold nanoparticles by many research groups and no interference has been reported [52–54]. Observed cytotoxicity of gold clusters depended on the surface chemistry of the clusters [55]. Goodman et al. show that cationic clusters are moderately toxic, whereas anionic clusters were not toxic [52]. As depicted in Fig. 4, a major cytotoxic effect was not observed for gold cluster treated C-26 cells. In vitro, radiosensitization studies were performed at 4 different concentrations and two doses (2 and 4 Gy) (Fig. 4b–c). With 2 Gy exposure to a Co-60 radiation beam, significant differences between gold cluster treated cells and untreated cells were observed in all concentrations but no significant difference between the control group and radiated group (0 µg/mL) was observed (Fig. 4b). With higher doses of Co-60 radiation, no significant difference was observed between treated and untreated cells (Fig. 4c).

Gold cluster concentration dependency of cell viability was observed in low doses treatment. Higher concentrations (128 and 256 µg/mL) of gold clusters led to lesser cell viability. This could be the result of gold cluster radiosensitization activity. Based on the provided results radiosensitization of the cancerous cell with Au cluster appears to be a promising technique for improved cancer treatment but further in vitro and in vivo investigations are necessary.

Doxorubicin and gold cluster loading efficacy

By increasing the initial gold concentration, the liposomal gold cluster loading increased but was not statistically significant. So in this range of concentrations, the average loading percentage of gold nanoclusters is about 14.3% and does not depend on the initial concentration of gold nanoclusters.

In comparison with passive loading techniques like hydration of dried lipid films with aqueous drug solutions, higher encapsulation efficiency is the main benefit of the remote loading procedure. Loading through an ammonium sulphate gradient is one of the most common remote loading techniques that have been employed for commercial stealth liposomal doxorubicin formulation [23]. Encapsulation efficiency in doxorubicin remote loading techniques is 98–100% [56], But in our experiments, the average percentage of doxorubicin loading is 63 ± 4.0 (Fig. 5). A high initial concentration of Au (1500 µg/mL) could decrease the final doxorubicin loading percentage (Significant differences have been observed (Fig. 5b). Decreasing in calcein passive loading because of gold nanoparticles presence in liposomes formulation was reported by Mathiyazhakan et al [36]. Similar results on the efficiency remote loading technique of

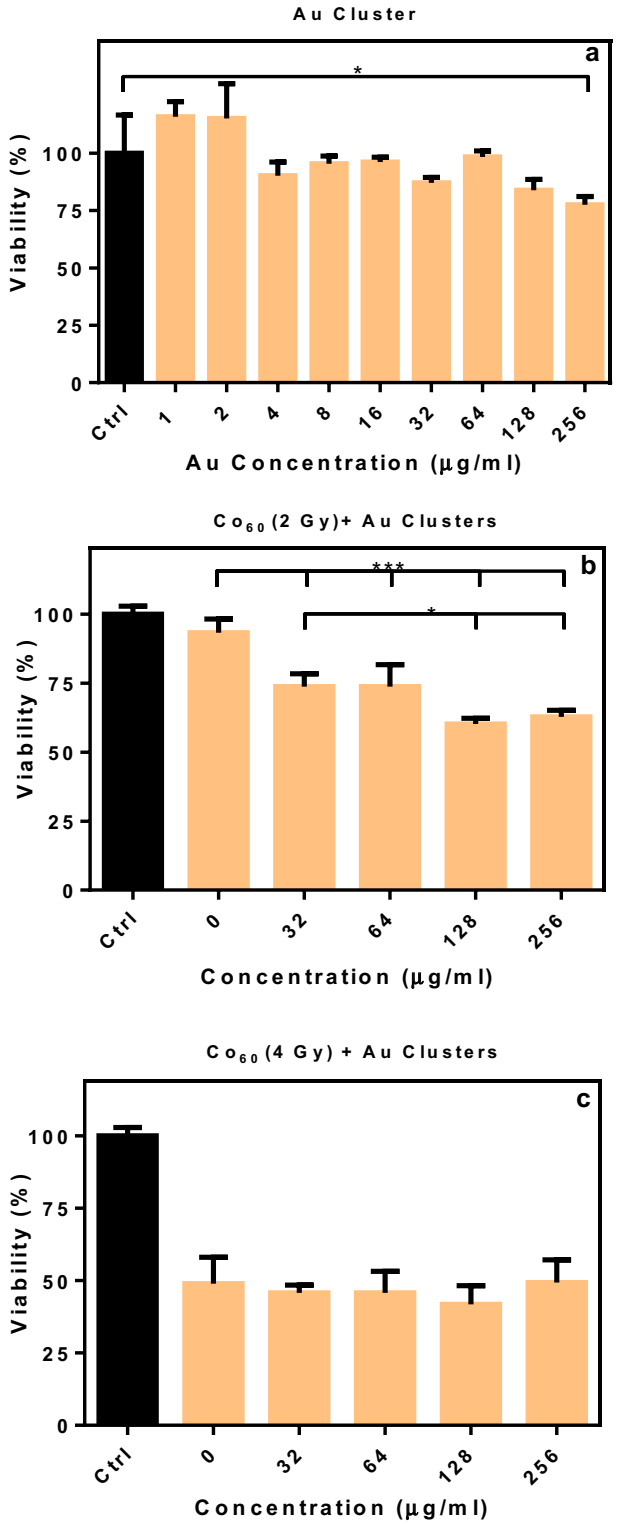

Fig. 4 Viability results based on MTT assay of colon carcinoma cells (CT26) with Au cluster treatment (**a**), Au clusters plus 2 Gy treatments (**b**), Au clusters plus 4 Gy treatments (**c**)

magnetic nanoparticles encapsulated liposomes have been observed by Pradhan et al. Doxorubicin loading in magnetic nanoparticles encapsulated liposomes were decreased by up to 85% whilst based on TEM micrographs that have been presented, the content of magnetic nanoparticle inside liposomes was very low [33].

Doxorubicin release at different temperatures

For investigating the temperature effect on doxorubicin release from gold cluster loaded liposomes, doxorubicin release in 4 different temperatures (1 h incubation) and with 3 different initial gold cluster concentrations was studied. Two-way analyses of variances have been used for statistical analysis investigation. In liposomes that have been prepared with 1500 µg/mL initial gold cluster concentration, there is no statistical difference between doxorubicin content inside liposomes in investigated temperatures. In liposomes with 1000 µg/mL initial gold cluster concentration, more than 20% of loaded doxorubicin was released after 1 h incubation in a 55 °C water bath. Liposomes with 500 µg/mL initial gold cluster concentration represent more than 25% doxorubicin release after 1 h 42 °C and 55 °C water bath incubation. The interactive effect of initial gold cluster concentration and incubation temperatures was statistically significant ($F(6, 24) = 3.88$, $P = 0.0145$) according to a two-way analysis of variance. Also, the mean effects of two variables were significant ($F(2, 24) = 19.66$, $P < 0.0001$ for incubation temperature, ($F(3, 24) = 19.86$, $P < 0.0001$ for initial Au concentration).

RF-EF stimulus doxorubicin release

Gold cluster encapsulated liposomes with an initial gold cluster concentration of 500 µg/mL was chosen for RF-EF stimulus doxorubicin release based on the release profile of 3 different formulations after one 1 h incubation in different temperature (Fig. 6). Stock solution (with initial 500 µg/mL gold cluster concentration) and a diluted solution of liposomes in 5% w/v dextrose with and without gold cluster were exposed to RF-EF (13.56 MHz, 100 Watt) for 3 min. Then the remaining doxorubicin content inside liposomes was studied (Fig. 7).

T-test analysis between RF-EF treated and not treated groups represent significant differences in remaining doxorubicin content for diluted solutions of both liposomes and gold cluster loaded liposomes. In RF-EF heating, joul heating of ionic background is very important [26, 57] and it should be considered for 5% w/v dextrose buffers. Increasing temperature as a result of joul heating of dextrose solution could be a major reason for the observed doxorubicin release profile for liposomes without gold clusters.

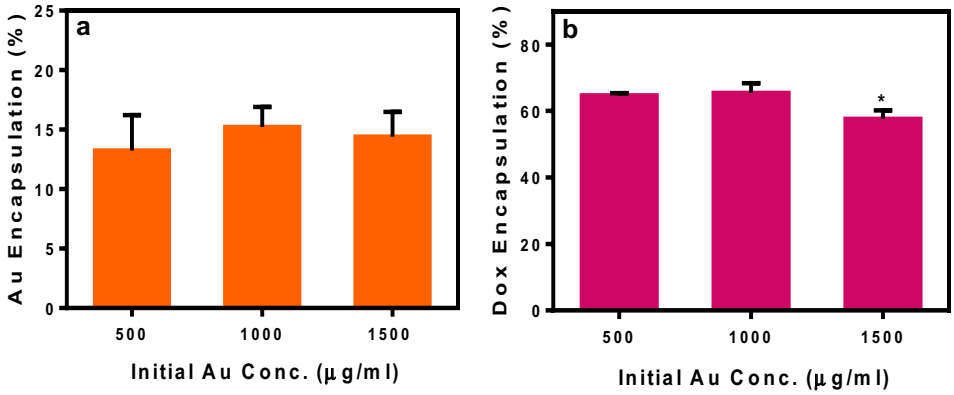

Fig. 5 Encapsulation efficiency of the gold cluster (**a**) and doxorubicin (**b**) in liposomes with different initial Au concentrations for liposomes preparation. One-way analysis of variance has been performed for statistical analysis of results (mean ± SD, $*P \leq 0.05$)

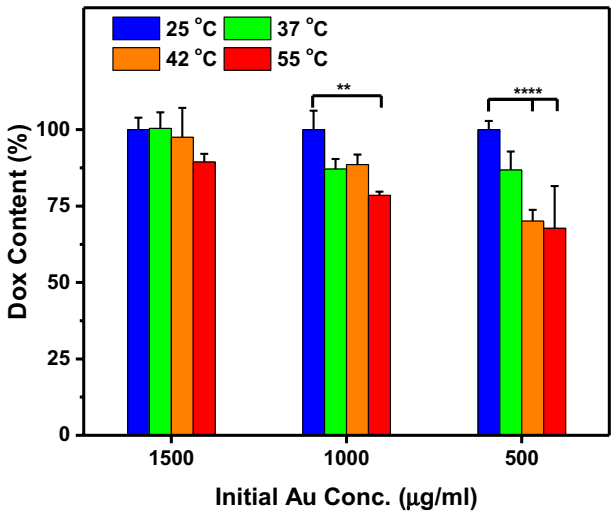

Fig. 6 Remaining Doxorubicin content of gold cluster loaded liposomes after 1 h water bath incubation in different temperatures. A two-way analysis of variance has been performed for statistical analysis of results (mean ± SD, $**P \leq 0.01$, $****P \leq 0.0001$)

Using a stock solution of gold cluster loaded liposomes with an initial 500 µg/mL Au concentration and a stock solution of liposomes without gold clusters leads to completely different results. T-test analysis between RF-EF treated and not treated groups represent significant differences in doxorubicin content only for liposomes which contain gold clusters.

Cytotoxicity analysis of gold cluster encapsulated liposomal doxorubicin

To investigate the impact of different doxorubicin treatments on cancer cells viability, colorectal carcinoma cells have been treated with gold cluster encapsulated liposomes containing doxorubicin (Au + Dox@Liposomes), Au + Dox@Liposomes after 3 min RF-EF exposure and free doxorubicin (Dox). As shown in Fig. 8, there was no significant

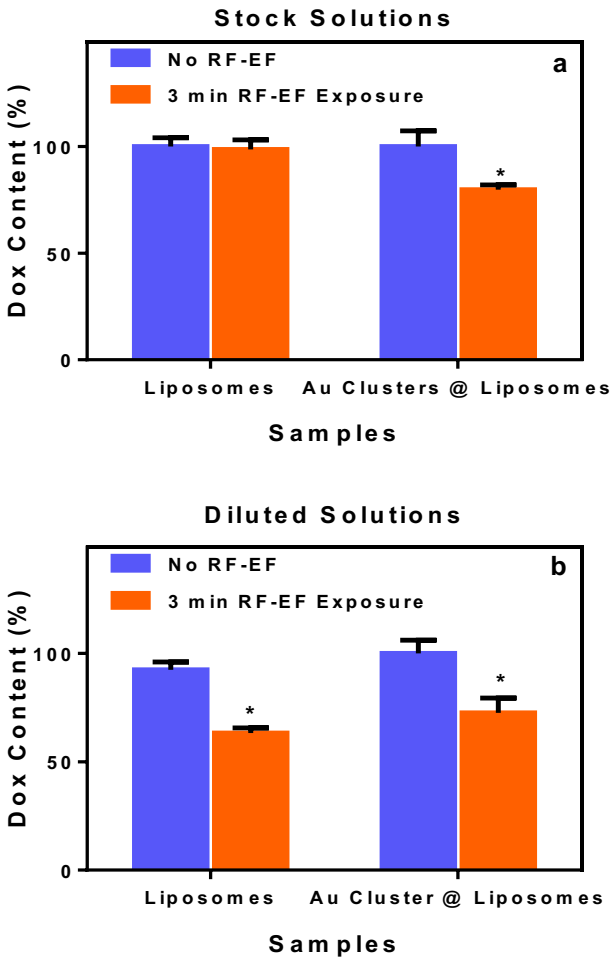

Fig. 7 Remaining Doxorubicin content of gold cluster encapsulated liposomes after 3 min RF-EF exposure for stock solution (**a**) and diluted solution (**b**). Student T-test analysis between RF-EF treated and not treated groups have been performed for statistical analysis of results (mean ± SD, $*P \leq 0.05$)

difference ($P > 0.05$) in the half maximal inhibitory concentration (IC50) between Au + Dox@Liposomes plus 3 min RF-EF exposure and Dox, but significant differences in IC50

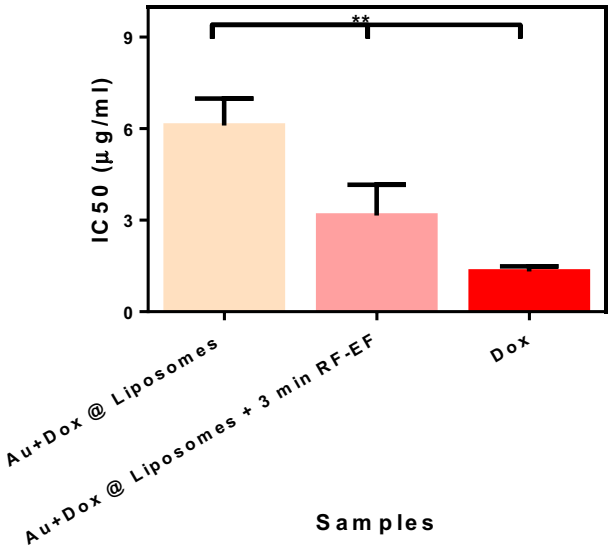

Fig. 8 Cytotoxicity profile of free and liposomal doxorubicin with encapsulated Au clusters against C-26 colon carcinoma cells. Cytotoxicity was measured by MTT assay (mean ± SD, $^{**}P \leq 0.01$)

values between cells that have been treated by Au + Dox@Liposomes with Dox and Au + Dox@Liposomes plus 3 RF-EF was observed, which is indicative of increased accessible and free doxorubicin drug for C-26 cells.

Conclusion

2 nm gold clusters represent good heating under RF-EF exposure and have been used for in vitro hyperthermia treatment of cancerous cells. Gold clusters encapsulated liposomal doxorubicin (169 ± 19.80 nm) were prepared and studied as a theranostic agent with high potential in different cancer treatment modalities. Exposure to a radiofrequency electric field on prepared formulation caused 20.2 ± 2.1% doxorubicin release and twice decreasing of IC50 on colorectal carcinoma cells. X-ray attenuation efficiency of the liposomal gold cluster was better than commercial iohexol and free gold clusters in different concentrations. Finally, treatment of gold clusters on cancerous cells results in a significant decrease in the viability of irradiated cells to cobalt-60 beam. However, the theranostic efficacy of gold clusters encapsulated liposomal doxorubicin was shown based on in vitro studies. Hence, in vivo antitumor investigations and also more molecular and pharmacological investigations must be conducted for the presented concept.

Acknowledgements This work has been funded by the Tehran University of Medical Sciences (93-01-87-25211). The authors are grateful to Dr. Hossein Ghadiri for providing the scanning holder for computed tomography experiments.

Funding Funding was provided by Tehran University of Medical Sciences and Health Services.

Declarations

Conflict of interest None.

References

1. DeAngelis LM, et al. Combination chemotherapy and radiotherapy for primary central nervous system lymphoma: Radiation Therapy Oncology Group Study 93–10. J Clin Oncol. 2002;20(24):4643–8.
2. Sriraman SK, Aryasomayajula B, Torchilin VP. Barriers to drug delivery in solid tumors. Tissue Barriers. 2014;2(3): e29528.
3. Fatemi F, et al. Construction of genetically engineered M13K07 helper phage for simultaneous phage display of gold binding peptide 1 and nuclear matrix protein 22 ScFv antibody. Colloids Surf B. 2017;159:770–80.
4. Koosha F, et al. Mesoporous silica coated gold nanorods: a multifunctional theranostic platform for radiotherapy and X-ray imaging. J Porous Mater. 2021;28(6):1961–8.
5. Neshastehriz A, et al. In-vitro investigation of green synthesized gold nanoparticle's role in combined photodynamic and radiation therapy of cancerous cells. Adv Nat Sci. 2020;11(4).
6. Kamalabadi M, et al. Folate functionalized gold-coated magnetic nanoparticles effect in combined electroporation and radiation treatment of HPV-positive oropharyngeal cancer. Med Oncol. 2022;39(12).
7. Baijal G, et al. Comparative study of one pot synthesis of PEGylated gold and silver nanoparticles for imaging and radiosensitization of oral cancers. Radiat Phys Chem. 2022;194: 109990.
8. Lin M-H, et al. Comparison of organic and inorganic germanium compounds in cellular radiosensitivity and preparation of germanium nanoparticles as a radiosensitizer. Int J Radiat Biol. 2009;85(3):214–26.
9. Porcel E, et al. Platinum nanoparticles: a promising material for future cancer therapy? Nanotechnology. 2010;21(8): 085103.
10. Shirkhanloo H, et al. Novel semisolid design based on bismuth oxide (Bi2O3) nanoparticles for radiation protection. Nanomed Res J. 2017;2(4):230–8.
11. Chithrani DB, et al. Gold nanoparticles as radiation sensitizers in cancer therapy. Radiat Res. 2010;173(6):719–28.
12. Zhang X-D, et al. In vivo renal clearance, biodistribution, toxicity of gold nanoclusters. Biomaterials. 2012;33(18):4628–38.
13. Khlebtsov N, Dykman L. Biodistribution and toxicity of engineered gold nanoparticles: a review of in vitro and in vivo studies. Chem Soc Rev. 2011;40(3):1647–71.
14. Hirn S, et al. Particle size-dependent and surface charge-dependent biodistribution of gold nanoparticles after intravenous administration. Eur J Pharm Biopharm. 2011;77(3):407–16.
15. Drummond DC, et al. Pharmacokinetics and in vivo drug release rates in liposomal nanocarrier development. J Pharm Sci. 2008;97(11):4696–740.
16. Drummond DC, et al. Optimizing liposomes for delivery of chemotherapeutic agents to solid tumors. Pharmacol Rev. 1999;51(4):691–744.
17. Halm U, et al. A phase II study of pegylated liposomal doxorubicin for treatment of advanced hepatocellular carcinoma. Ann Oncol. 2000;11(1):113–4.
18. Chidiac T, et al. Phase II trial of liposomal doxorubicin (Doxil®) in advanced soft tissue sarcomas. Invest New Drugs. 2000;18(3):253–9.

19. Laginha KM, et al. Determination of doxorubicin levels in whole tumor and tumor nuclei in murine breast cancer tumors. Clin Cancer Res. 2005;11(19):6944–9.
20. Tseng Y-L, Liu J-J, Hong R-L. Translocation of liposomes into cancer cells by cell-penetrating peptides penetratin and tat: a kinetic and efficacy study. Mol Pharmacol. 2002;62(4):864–72.
21. Ng K-Y, et al. The effects of polyethyleneglycol (PEG)-derived lipid on the activity of target-sensitive immunoliposome. Int J Pharm. 2000;193(2):157–66.
22. Parr MJ, et al. Accumulation of liposomal lipid and encapsulated doxorubicin in murine Lewis lung carcinoma: the lack of beneficial effects by coating liposomes with poly (ethylene glycol). J Pharmacol Exp Ther. 1997;280(3):1319–27.
23. Allen TM, Cullis PR. Liposomal drug delivery systems: from concept to clinical applications. Adv Drug Deliv Rev. 2013;65(1):36–48.
24. Biabangard A, et al. Study of FA12 peptide-modified PEGylated liposomal doxorubicin (PLD) as an effective ligand to target Muc1 in mice bearing C26 colon carcinoma: in silico, in vitro, and in vivo study. Expert Opin Drug Deliv. 2022;19(12):1710–24.
25. Bibi S, et al. Trigger release liposome systems: local and remote controlled delivery? J Microencapsul. 2012;29(3):262–76.
26. Amini SM, Kharrazi S, Jaafari MR. Radio frequency hyperthermia of cancerous cells with gold nanoclusters: an in vitro investigation. Gold Bull. 2017;50(1):43–50.
27. Amin M, Badiee A, Jaafari MR. Improvement of pharmacokinetic and antitumor activity of PEGylated liposomal doxorubicin by targeting with N-methylated cyclic RGD peptide in mice bearing C-26 colon carcinomas. Int J Pharm. 2013;458(2):324–33.
28. Bartlett GR. Phosphorus assay in column chromatography. J Biol Chem. 1959;234:466–8.
29. Bolotin EM, et al. Ammonium sulfate gradients for efficient and stable remote loading of amphipathic weak bases into liposomes and ligandoliposomes. J Liposome Res. 1994;4(1):455–79.
30. Haran G, et al. Transmembrane ammonium sulfate gradients in liposomes produce efficient and stable entrapment of amphipathic weak bases. Biochim Biophys Acta. 1993;1151(2):201–15.
31. Huang Z, Jaafari MR, Szoka FC Jr. Disterolphospholipids: nonexchangeable lipids and their application to liposomal drug delivery. Angew Chem. 2009;121(23):4210–3.
32. Siegel MJ, et al. Radiation dose and image quality in pediatric CT: effect of technical factors and phantom size and shape 1. Radiology. 2004;233(2):515–22.
33. Pradhan P, et al. Targeted temperature sensitive magnetic liposomes for thermo-chemotherapy. J Control Release. 2010;142(1):108–21.
34. Lorenzato C, et al. MRI contrast variation of thermosensitive magnetoliposomes triggered by focused ultrasound: a tool for image-guided local drug delivery. Contrast Media Mol Imaging. 2013;8(2):185–92.
35. Zarchi AAK, et al. Synthesis and characterisation of liposomal doxorubicin with loaded gold nanoparticles. IET Nanobiotechnol. 2018;12:846–9.
36. Mathiyazhakan M, et al. Non-invasive controlled release from gold nanoparticle integrated photo-responsive liposomes through pulse laser induced microbubble cavitation. Colloids Surf B. 2015;126:569–74.
37. Xia Y, et al. Construction of thermal-and light-responsive liposomes noncovalently decorated with gold nanoparticles. RSC Adv. 2014;4(84):44568–74.
38. Demir B, et al. Gold nanoparticle loaded phytosomal systems: synthesis, characterization and in vitro investigations. RSC Adv. 2014;4(65):34687–95.
39. Freeny PC, et al. Colorectal carcinoma evaluation with CT: preoperative staging and detection of postoperative recurrence. Radiology. 1986;158(2):347–53.
40. Rifkin MD, Ehrlich S, Marks G. Staging of rectal carcinoma: prospective comparison of endorectal US and CT. Radiology. 1989;170(2):319–22.
41. Lusic H, Grinstaff MW. X-ray-computed tomography contrast agents. Chem Rev. 2012;113(3):1641–66.
42. Hainfeld, J., et al. Gold nanoparticles: a new X-ray contrast agent. Br J Radiol 2014.
43. Rabin O, et al. An X-ray computed tomography imaging agent based on long-circulating bismuth sulphide nanoparticles. Nat Mater. 2006;5(2):118–22.
44. Kandanapitiye MS, et al. Synthesis, characterization, and X-ray attenuation properties of ultrasmall BiOI nanoparticles: toward renal clearable particulate CT contrast agents. Inorg Chem. 2014;53(19):10189–94.
45. Liu Z, et al. Long-circulating Er 3+-doped Yb 2 O 3 up-conversion nanoparticle as an in vivo X-Ray CT imaging contrast agent. Biomaterials. 2012;33(28):6748–57.
46. Liu Y, et al. A high-performance ytterbium-based nanoparticulate contrast agent for in vivo X-ray computed tomography imaging. Angew Chem Int Ed. 2012;51(6):1437–42.
47. Lechtman E, et al. Implications on clinical scenario of gold nanoparticle radiosensitization in regards to photon energy, nanoparticle size, concentration and location. Phys Med Biol. 2011;56(15):4631.
48. Khoshgard K, et al. Radiosensitization effect of folate-conjugated gold nanoparticles on HeLa cancer cells under orthovoltage superficial radiotherapy techniques. Phys Med Biol. 2014;59(9):2249.
49. Hainfeld JF, et al. Radiotherapy enhancement with gold nanoparticles. J Pharm Pharmacol. 2008;60(8):977–85.
50. Leung MK, et al. Irradiation of gold nanoparticles by x-rays: Monte Carlo simulation of dose enhancements and the spatial properties of the secondary electrons production. Med Phys. 2011;38(2):624–31.
51. Hill R, et al. Advances in kilovoltage X-ray beam dosimetry. Phys Med Biol. 2014;59(6):R183.
52. Goodman CM, et al. Toxicity of gold nanoparticles functionalized with cationic and anionic side chains. Bioconjug Chem. 2004;15(4):897–900.
53. Marquis BJ, et al. Analytical methods to assess nanoparticle toxicity. Analyst. 2009;134(3):425–39.
54. Niidome T, et al. PEG-modified gold nanorods with a stealth character for in vivo applications. J Control Release. 2006;114(3):343–7.
55. Mathew A, Pradeep T. Noble metal clusters: applications in energy, environment, and biology. Part Part Syst Charact. 2014;31(10):1017–53.
56. Mayer L, Bally M, Cullis P. Uptake of adriamycin into large unilamellar vesicles in response to a pH gradient. Biochim Biophys Acta. 1986;857(1):123–6.
57. Hanson GW, Monreal R, Apell SP. Electromagnetic absorption mechanisms in metal nanospheres: Bulk and surface effects in radiofrequency-terahertz heating of nanoparticles. J Appl Phys. 2011;109(12): 124306.